

Photoionization of group-II*B* elements

W. R. Johnson, V. Radojević,* and Pranawa Deshmukh

Department of Physics, University of Notre Dame, Notre Dame, Indiana 46556

K. T. Cheng

Argonne National Laboratory, Argonne, Illinois 60439

(Received 17 July 1981)

Theoretical photoionization cross sections, angular distributions, and spin-polarization parameters for outer ns and $(n-1)d$ subshells of the group-II*B* elements zinc, cadmium, and mercury are determined above their respective $(n-1)d$ thresholds. Account is taken of electron-electron correlation and of the spin-orbit interaction by means of the relativistic random-phase approximation. Comparisons are made with previous theoretical work and with available experimental measurements.

I. INTRODUCTION

In the paragraphs below we present the results of a theoretical study of photoionization of outer ns and $(n-1)d$ electrons for the group-II*B* elements zinc, cadmium, and mercury. These studies were made using the relativistic random-phase approximation (RRPA) (Ref. 1) which takes into account many of the important aspects of electron-electron correlation, including coupling between the various photoionization channels, and which also accounts for the spin-orbit interaction. We limit the present study to photon energies above the respective $(n-1)d_{3/2}$ thresholds to avoid complications arising from autoionization resonances at lower photon energies.

During the past decade a number of theoretical investigations of photoionization of group-II *B* elements in the energy range of interest have appeared. Predictions of the $3d$ cross section of zinc which include correlations have been made by Amusia and Cherepkov² using the nonrelativistic random-phase approximation with exchange (RPAE), and by Fliflet and Kelly³ using the many-body perturbation theory (MBPT). Carter and Kelly⁴ have reported nonrelativistic MBPT calculations of the cross section and angular distribution asymmetry parameter β for $4d$ electrons in cadmium. To date no nonrelativistic correlated calculations have been published for mercury, however, Keller and Combet-Farnoux⁵ have determined the mercury $5d$ cross section in the Hartree-Slater (HS) approximation.

The importance of relativistic (spin-orbit) effects in mercury was pointed out by Walker *et al.*⁶ who determined partial cross sections and angular distributions for $5d$ electrons in mercury using the Dirac-Slater approximation. More recently Tamba *et al.*⁷ and Theodosiou *et al.*⁸ have completed Dirac-Fock (DF) calculations for both cadmium and mercury.

On the experimental side there have been measurements of cross sections employing atomic beams; for zinc by Harrison *et al.*,⁹ and for zinc, cadmium, and mercury by Cairns *et al.*^{10,11} Absolute cross sections for cadmium have been measured by Codling *et al.*¹² using a heat-pipe absorption cell and a synchrotron light source. Line sources have been employed to determine partial cross sections for $5d$ electrons as well as total cross sections for mercury by Dehmer and Berkowitz¹³; and to determine partial cross sections for zinc, cadmium, and mercury by Süzer *et al.*¹⁴ Partial cross-section measurements for cadmium and mercury have also been made by Shannon and Codling¹⁵ using synchrotron radiation.

The angular distribution asymmetry parameters β for ns and $(n-1)d$ subshells of zinc and cadmium have been measured at several wavelengths by Harrison¹⁶; and for mercury by Niehaus and Ruf.¹⁷ More recently Schönhense¹⁸ has measured the β parameters for $4d$ electrons in cadmium and for $5d$ electrons in mercury, and Schönhense *et al.*¹⁹ have determined β for the $6s$ electron in mercury at several wavelengths.

Little attention has been given to the spin-

polarization parameters of group-II B atoms despite the fact that these parameters are sensitive to both correlation and relativistic effects. Two notable exceptions are the measurements of transverse spin polarization of the $6s$ electron in mercury at several wavelengths by Schönhense *et al.*,¹⁹ and for $5d$ electrons in mercury by Schönhense.²⁰ No theoretical studies of spin polarization of photoelectrons for group-II B elements have been reported.

In view of the recent interest in group-II B elements by both theorists and by experimentalists it seems appropriate to present a theoretical survey of cross sections, angular distributions, and spin-polarization parameters for these elements from a unified point of view. This survey should help in identifying potentially important measurements, and in understanding the limitations of the atomic theory employed.

In the present calculations we use a truncated version of the RRPA in which only excitations of ns and $(n-1)d$ electrons are considered. We work in dipole approximation and include eight coupled channels:

$$ns_{1/2} \rightarrow p_{1/2}, p_{3/2},$$

$$(n-1)d_{3/2} \rightarrow p_{1/2}, p_{3/2}, f_{5/2},$$

$$(n-1)d_{5/2} \rightarrow p_{3/2}, f_{5/2}, f_{7/2}.$$

The RRPA equations are solved for the dipole amplitudes in each of the eight channels and these dipole amplitudes are then combined to give the measurable photoionization parameters.

We ignore excitations of $(n-1)p$, and other tightly bound electrons. Contributions from excitation channels of the $(n-1)p$ subshells are found

to be negligibly small in the energy region considered here. A minor problem which occurs when we truncate the RRPA equations is the loss of gauge independence, which has the consequence that dipole amplitudes have different values in length form and in velocity form. We find, nevertheless, that the two forms, length and velocity, agree to within a few percent throughout the energy range considered.

The thresholds usually employed in the RPA-type calculations are HF eigenvalues.² These theoretical thresholds differ from the experimental thresholds because of the many-body effects not included in RPA calculations. As has been discussed by Kelly,²¹ and by Carter and Kelly,⁴ certain many-body effects omitted in RPA calculations may be accounted for empirically by employing experimental removal energies rather than HF eigenvalues. In the present calculations we employ this semiempirical procedure, replacing DF eigenvalues by experimental removal energies²² listed in Table I.

The potentially important effects of core relaxation⁴ are not included in the present calculation. In this regard it may be noted that some calculations including core relaxation effects by Amusia and Cherepkov² indicated improvement of agreement between theoretical and experimental values of the cross section for argon near the threshold. We also neglect the effects of two electron excitations which are responsible for the appearance of correlation satellites²³ in the photoelectron spectra of group-II B elements.

In Sec. II we present our results for total and partial cross sections and we make comparisons with previous work. In Sec. III we give our values for the angular distribution β parameters for ns

TABLE I. Experimental removal energies and theoretical Dirac-Fock (DF) eigenvalues (a.u.) for ns and $(n-1)d$ electrons of group-II B elements.

Atom	Subshell	Exp. ^a	DF
Zn	$4s_{1/2}$	0.3452	0.2986
	$3d_{5/2}$	0.6310	0.7547
	$3d_{3/2}$	0.6434	0.7709
Cd	$5s_{1/2}$	0.3305	0.2814
	$4d_{5/2}$	0.6461	0.7089
	$4d_{3/2}$	0.6718	0.7382
Hg	$6s_{1/2}$	0.3836	0.3281
	$5d_{5/2}$	0.5454	0.5746
	$5d_{3/2}$	0.6139	0.6500

^aMoore, Reference 22.

and $(n-1)d$ electrons, then in Sec. IV, we present results for the spin-polarization parameters. In Sec. V we summarize the conclusions which we draw from comparisons with previous work.

II. CROSS SECTIONS

The eight ionization channels in our calculation are conveniently labeled by the quantum numbers n and j of the atomic subshell being ionized and the angular momentum $j' = j, j \pm 1$ of the resulting continuum electron. The partial cross section for photoionizing an electron from subshell (n, j) is given by¹

$$\sigma_{nj} = \frac{4\pi^2\alpha}{3} \omega (|D_{nj,j-1}|^2 + |D_{nj,j}|^2 + |D_{nj,j+1}|^2), \quad (2.1)$$

where ω is the photon energy and where $D_{nj,j'}$ is the dipole amplitude for channel (nj, j') . We employ atomic units throughout the calculation. The three partial cross sections of interest here are for electrons in the $ns_{1/2}$, $(n-1)d_{3/2}$, and $(n-1)d_{5/2}$ subshells.

In Fig. 1 we present our calculated total cross sections $s_{1/2} + (n-1)d_{3/2} + (n-1)d_{5/2}$ for the group-II B elements. The solid curves give the RRPA predictions, while the remaining lines give the results of Tamm-Dancoff (TD) calculations carried out using length and velocity forms, respectively, for the dipole amplitudes. The TD amplitudes themselves are determined from fully coupled relativistic calculations which have all the features of RRPA except that the effects of ground-state correlations are neglected.²³ It should be mentioned that when interchannel coupling is also omitted the TD amplitudes reduce to DF amplitudes.

There are characteristic similarities in the cross

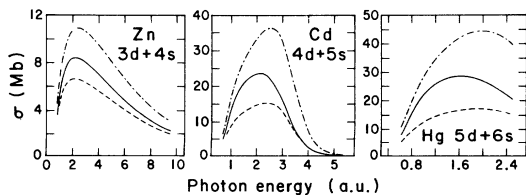


FIG. 1. Total cross sections: RRPA —; TD (length-form) - - - -; and TD (velocity-form) - - - - cross sections are compared above the respective $(n-1)d$ thresholds. Contribution from ns and $(n-1)d$ subshells are included.

sections for all of the group-II B elements; the cross sections rise steadily from the threshold [due to centrifugal barrier effects on the dominant $(n-1)d \rightarrow f$ orbital wave functions] and after reaching a maximum near 2 a.u. they gradually decrease.

In Fig. 2 we show the $(n-1)d_{3/2}$ and $(n-1)d_{5/2}$ partial cross sections together with the total $(n-1)d$ cross section determined from the RRPA calculations. The present RRPA calculations for zinc are in excellent agreement with the RPAE calculations of Amusia and Cherepkov² and with the MBPT calculations of Fliflet and Kelly.³ The cadmium $4d$ cross section is in good agreement with the unrelaxed calculation of Carter and Kelly⁴ in which second-order ground-state correlations were included (GMS), but as we shall discuss below, the RRPA cross section is significantly larger than the Carter and Kelly⁴ calculation in which the second-order ground-state correlations were omitted and relaxation effects were included (GMR). The mercury $5d$ partial cross sections agree well with the measurements of Shannon and Codling¹⁵ near threshold but the present results are significantly larger than the experimental values at higher energies. For comparison we also present the experimental total cross section for mercury, determined by Dehmer and Berkowitz¹³ which is accurate to $\pm 30\%$, and the DF results of Tambe *et al.*⁷ The discrepancy with experiment may reflect the importance of relaxation effects or may be due to difficulties associated with absolute cross-section measurements. The differences between the RRPA and DF calculations will be discussed in the following paragraph.

For cadmium absolute-cross-section measurements accurate to $\pm 20\%$ are available in the 40–250-eV energy range from the work of Co-

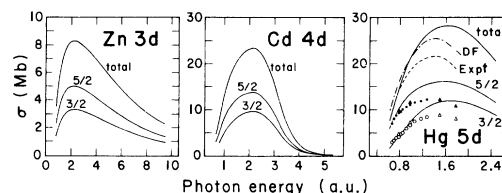


FIG. 2. Partial $(n-1)d$ cross sections: RRPA cross sections for $(n-1)d_{5/2}$ and $(n-1)d_{3/2}$ subshells are given together with the total $(n-1)d$ values. Full coupling within $(n-1)d$ subshells and coupling with the ns subshell is included. Hg experimental cross sections: Expt. - - -, \blacktriangle , \triangle Dehmer and Berkowitz, Ref. 13; \bullet , \circ Shannon and Codling, Ref. 15. Hg DF calculation: - - - - Tambe *et al.*, Ref. 7.

dling *et al.*¹² The RRPA cross section is compared with these measurements, with the MBPT-GMR results of Carter and Kelly,⁴ and with the DF calculations of Tambe *et al.*⁷ in Fig. 3. One significant difference between the present calculation and the GMR calculations is that the effects of core relaxation are included in the GMR but not in the RRPA. According to Carter and Kelly relaxation reduces the maximum cross sections and shifts the maximum toward higher energy. The DF calculations of Tambe *et al.* (which were carried out in the velocity gauge) take similar relaxation effects into account. These DF calculations also lead to cross sections smaller than those predicted by RRPA; however, the DF calculations, like the TD calculations described above depend on the gauge of the photon field. Judging from the comparison of the TD (velocity-form) and TD (length-form) results shown in Fig. 1, one would expect a length gauge DF calculation to give cross sections considerably larger than the RRPA values.

The branching ratio of the $(n-1)d$ partial cross sections $\gamma = (n-1)d_{5/2} : (n-1)d_{3/2}$ is shown in Fig. 4. Nonrelativistically this ratio reduces to the statistical ratio, $\gamma = 1.5$, of the ground-state orbital occupation numbers. Relativistically spin-orbit interaction lifts the l degeneracy and causes γ to depart from the statistical ratio. For the $3d$ branching ratio of zinc there is a noticeable spin-orbit effect near threshold with γ predicted to be greater than 1.5 but measured^{6,14,24} to be less than or equal to 1.5. In cadmium there is again a large near-threshold effect on the $4d$ branching ratio predicted theoretically, in fair agreement with the experimental measurements.^{14,15,24} We also show the DF results of Tambe *et al.*⁷ for cadmium which have the same general shape near threshold as the RRPA calculations but which show a some-

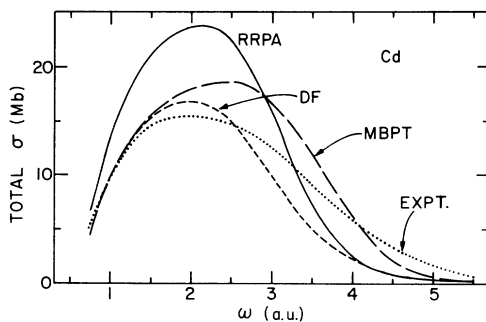


FIG. 3. RRPA total cross section for cadmium compared with other works. Experiment: Codling *et al.*, Ref. 12. Theory: MBPT, Carter and Kelly, Ref. 4; DF, Tambe *et al.*, Ref. 7.

what smaller departure from the statistical ratio. At higher energies near the $4d$ "Cooper" minimum of the cadmium cross section there is a dip in the RRPA value of γ caused by the fact that the $4d_{5/2} \rightarrow f_{7/2}$ amplitude reaches its minimum before the $4d_{3/2} \rightarrow f_{5/2}$ amplitude. The sizable discrepancy with the DF calculations in cadmium at higher energies may be due to the importance of inter-channel coupling which is omitted in the DF calculations. In the third panel of Fig. 4 we compare the $5d$ branching ratio of mercury with experimental values^{13-15,24} and with the DF calculations of Tambe *et al.*⁷ Except for the increase in size of the spin-orbit effect the comparisons for the mercury $5d$ subshells closely parallel those made for the cadmium $4d$ subshells. We note that despite the rather large discrepancy between cross-section measurements and RRPA for cadmium and mercury the branching ratios agree quite well.

The behavior of the $ns_{1/2}$ cross section is illustrated in the solid curves of Fig. 5. In the absence of coupling with the $5d$ subshell in mercury, an HS calculation has shown that the $6s$ cross section decreases from the $6s$ threshold to a Cooper minimum slightly above the $5d$ threshold.¹³ By contrast, when couplings with the $5d$ subshells are included in the present calculation, the $6s$ cross section rises sharply above the $5d$ threshold; the shape of the cross section being determined principally by the interchannel coupling with the $5d \rightarrow f$ amplitudes. This sharp rise causes the $6s$ cross-section Cooper minimum to be shifted below the $5d$ threshold. Similar features are common to the ns cross sections of all three atoms.

For comparison we also show in Fig. 5 the results of TD calculations and note the disparity between the length and velocity gauge predictions, regarding both the overall size and the shape of the ns cross sections. We also include in the last panel of Fig. 5 the values measured by Shannon and Codling²⁵ for the mercury $6s$ cross section. It should be noted that the experimental $6s$ cross section shows a minimum near 0.7 a.u., in the region above the $5d$ threshold, at variance with the RRPA prediction.

Another interesting feature of the present calculation is the appearance of a second Cooper minimum in the cadmium $5s$ cross section near 4 a.u. This minimum leads to rapid variations in the β parameters and spin-polarization parameters, as we shall show in the following paragraphs. It is interesting to point out that the $6s$ cross section in mercury seems to approach a similar minimum

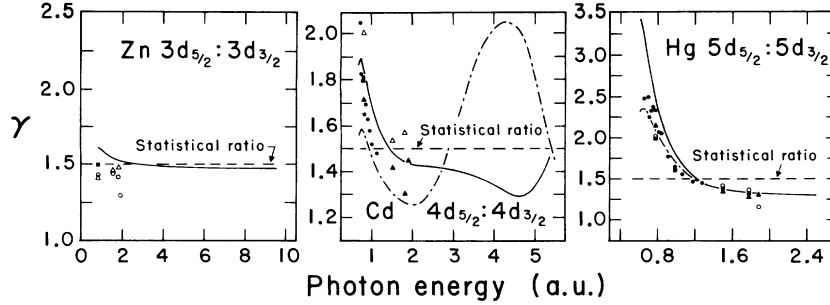


FIG. 4. Branching ratios for $(n-1)d$ subshells. RRPAs: —, predictions are compared with other works. Zn: ■ Walker *et al.*, Ref. 6; ○ Süzer *et al.*, Ref. 14; △ Süzer *et al.*, Ref. 24. Cd: ■ Walker *et al.*, Ref. 6; ● Shannon and Codling, Ref. 15; ▲ Süzer *et al.*, Ref. 14; △ Süzer *et al.*, Ref. 24. Hg: ■ Dehmer and Berkowitz, Ref. 13; ● Shannon and Codling, Ref. 15; ○ Süzer *et al.*, Ref. 14; ▲ Süzer *et al.*, Ref. 24. DF calculations for Cd, Hg: - - - - Tambe *et al.*, Ref. 7.

above 2.5 a.u. However, this minimum is very close to the $5p$ threshold and it is difficult to pinpoint its location.

III. ANGULAR DISTRIBUTIONS

In the dipole approximation the differential cross section for photoionizing an electron from a subshell (n, j) by unpolarized radiation of energy ω is given by¹

$$\frac{d\sigma_{nj}}{d\Omega} = \frac{\sigma_{nj}(\omega)}{4\pi} \left[1 - \frac{1}{2} \beta_{nj}(\omega) P_2(\cos\theta) \right], \quad (3.1)$$

where θ is the angle between the direction of the outgoing photoelectron and the direction of the incident radiation. The angular distribution asymmetry parameter $\beta_{nj}(\omega)$ may easily be determined in terms of the dipole amplitudes $D_{nj,j}$.¹

The RRPAs predictions for the β parameters of $(n-1)d_{3/2}$ and $(n-1)d_{5/2}$ photoelectrons are shown in Fig. 6. In the first panel we give the zinc $3d$ angular distribution; there is no difference

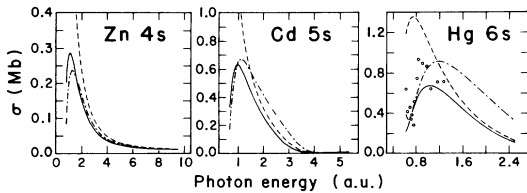


FIG. 5. Partial cross sections for ns subshells: RRPAs —, TD (length-form) - · - · - ·; TD (velocity-form) - - - cross sections are compared above the $(n-1)d$ thresholds. Full coupling with the $(n-1)d$ channels is included. Experiment: ○ Shannon and Codling, Ref. 15.

on the scale of the figure between the $3d_{3/2}$ and $3d_{5/2}$ values. There is a small but noticeable difference between the $4d_{3/2}$ and $4d_{5/2}$ predictions in cadmium shown in the second panel, where comparison is made with the angular distribution measurements of Schönense.¹⁸ The experimental and theoretical determinations are seen to be in relatively good agreement. The third panel illustrates the increased role of the spin-orbit interaction in mercury; the various experimental^{17,18} measurements are again in good agreement with the RRPAs.

In Fig. 7 we compare the RRPAs calculations of β for cadmium with the MBPT predictions of Carter and Kelly⁴ and with the DF calculations of Theodosiou *et al.*⁸ Since the MBPT calculations do not account for the spin-orbit interaction there is no distinction between $d_{3/2}$ and $d_{5/2}$ values. the DF curves of Theodosiou *et al.*⁸ have the same general energy dependence as the RRPAs curves but show a larger spin-orbit splitting, possibly because the DF calculations employed uncoupled jj amplitudes.

The angular distribution parameters for ns elec-

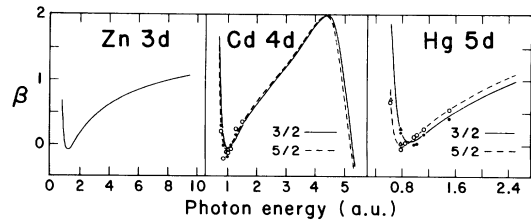


FIG. 6. Angular distribution asymmetry parameters β for $(n-1)d$ subshells. Experiment, Cd: ○ $d_{5/2}$, ● $d_{3/2}$; Schönense, Ref. 18; Hg: ○ $d_{5/2}$, ● $d_{3/2}$; Schönense, Ref. 18; △ $d_{5/2}$, ▲ $d_{3/2}$; Niehaus and Ruf, Ref. 17.

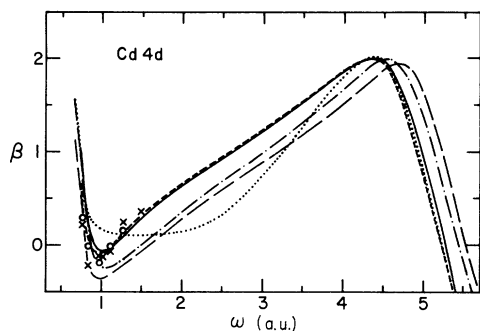


FIG. 7. Angular distribution asymmetry parameters for $4d_{3/2}$ — and $4d_{5/2}$ - - - subshells of cadmium are compared with other work. Theory: \cdots Carter and Kelly, Ref. 4; Theodosiou *et al.*, - - - - $4d_{5/2}$, - - - $4d_{3/2}$, Ref. 8. Experiment: \times $d_{5/2}$, \circ $d_{3/2}$ Schönhense, Ref. 18.

trons are shown in Fig. 8. Nonrelativistically the value of β is predicted to have the value 2 for an ns electron at all energies. In relativistic calculations there are two excitation channels corresponding to $ns_{1/2} \rightarrow p_{1/2}, p_{3/2}$. The amplitudes in these two channels can be combined in LS coupling to give a singlet amplitude D_1 which is the generalization of the single nonrelativistic amplitude and a triplet amplitude D_3 which has no counterpart in the nonrelativistic theory. The value of β relativistically is²⁶

$$\beta = 2 - 3 |D_3|^2 / (|D_1|^2 + |D_3|^2). \quad (3.2)$$

For outer shells D_1 is ordinarily much larger than D_3 so that β stays near 2; however, near a nonrelativistic Cooper minimum where D_1 is close to zero, β can depart from 2. For zinc the $4s$ β parameter takes on its nonrelativistic value of 2 throughout the entire range of energies considered. The cadmium $5s$ β parameter also stays near 2 except near the $5s$ cross-section minimum near 4 a.u. For mercury the situation is more interesting. Near the $5d$ threshold the $6s$ β parameter shows a strong depar-

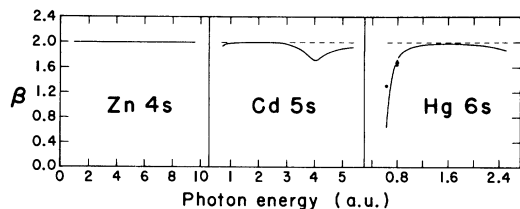


FIG. 8. Angular distribution asymmetry parameters β for ns subshells. Experiment: \bullet Schönhense *et al.*, Ref. 19; Δ Niehaus and Ruf, Ref. 17.

ture from 2 reflecting the fact that the RRPA $6s$ Cooper minimum occurs below the $5d_{3/2}$ threshold. The theoretical values are in general agreement with the measurements of Schönhense *et al.*¹⁹ and of Niehaus and Ruf.¹⁷ If the $6s$ Cooper minimum is above the $d_{3/2}$ threshold as indicated by the cross-section measurements of Shannon and Codling,¹⁵ then as pointed out by Schönhense, *et al.*,¹⁹ the $6s$ β parameter would have a minimum above the $d_{3/2}$ threshold. The fall off of β_{6s} at higher energy is indicative of a second minimum in the $6s$ cross section occurring beyond the range of energies considered here.

IV. SPIN POLARIZATION

For circularly polarized incident radiation the spin orientation of the outgoing photoelectrons is polarized with respect to the direction of the incident radiation \vec{k} and the direction of this outgoing photoelectron \vec{p} .²⁷⁻²⁹ If we choose a coordinate system with the z axis along \vec{p} , with the y axis in the direction $\vec{k} \times \vec{p}$, and with the x axis in the direction $[\vec{k} \times \vec{p}] \times \vec{p}$, then the components of the spin-polarization vector are²⁷

$$P_x = \pm \xi \sin \theta / F(\theta), \quad (4.1)$$

$$P_y = \eta \sin \theta \cos \theta / F(\theta), \quad (4.2)$$

$$P_z = \pm \zeta \cos \theta / F(\theta), \quad (4.3)$$

with

$$F(\theta) = 1 - \frac{1}{2} \beta P_2(\cos \theta). \quad (4.4)$$

Here the \pm signs refer to incident radiation with helicity ± 1 , respectively, and θ is the angle between \vec{k} and \vec{p} defined previously. In Eqs. (4.1)–(4.3) the parameters ξ, η, ζ (in the notation of Huang²⁷) are dimensionless dynamical quantities which are given in terms of the dipole amplitudes $D_{nj,j}$.²⁷ For comparison, we note that the spin-polarization parameters (ξ, η, ζ) are related to those of Lee²⁸ $(\delta_k, \xi_k, \gamma_k)$ by $\xi = -\delta_k$, $\eta = 2\xi_k$, $\zeta = \gamma_k$. The spin polarization of the total photoelectron flux is along the direction \vec{k} and has the value

$$P_{\text{tot}} = \pm \delta, \quad (4.5)$$

where

$$\delta = (\zeta - 2\xi) / 3. \quad (4.6)$$

Figure 9 gives the results of the RRPA calculations for the $(n-1)d$ spin-polarization parameters for the group-IIIB elements. The $3d$ parameters for

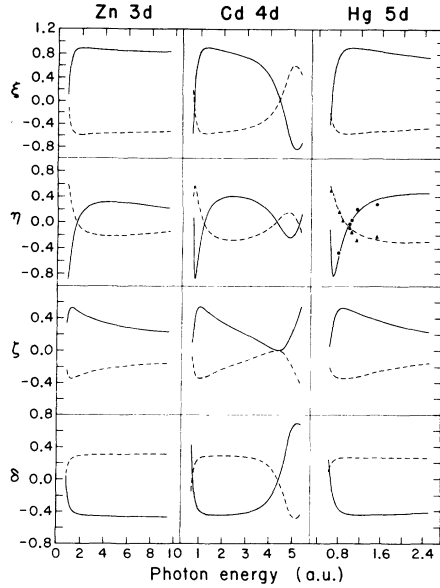


FIG. 9. Spin-polarization parameters for $(n-1)d$ subshells. Notation is that of Huang, Ref. 27. --- $d_{5/2}$, — $d_{3/2}$. Experiment: Δ $d_{5/2}$, \bullet $d_{3/2}$ Schönhense, Ref. 30.

zinc show the expected nonrelativistic dependence on j , viz.,

$$\xi_{5/2}:\xi_{3/2}=\eta_{5/2}:\eta_{3/2}=\zeta_{5/2}:\zeta_{3/2}=-2:3. \quad (4.7)$$

The features appearing near threshold for zinc are due to interference between the rapidly changing $3d \rightarrow f$ and $3d \rightarrow p$ amplitudes. The $4d$ parameters for cadmium are similar to zinc $3d$ parameters near threshold, but we observe small shifts in the $4d$ curves due to the fine structure of the two $4d$ thresholds. At higher energies near the $4d$ Cooper minimum at 4.5 a.u. there is an additional strong energy dependence in the $4d$ parameters caused by the near vanishing of the $4d \rightarrow f$ amplitudes. The general pattern of the $5d_{3/2}$ parameters is similar to that predicted for the zinc $3d_{3/2}$ and cadmium $4d_{3/2}$ parameters. For the $5d_{5/2}$ subshell, however, the threshold behavior of the transverse spin polarization is caused by sizable spin-orbit effects on the dipole amplitudes. The predicted behavior of the transverse spin-polarization parameters for mercury are seen to be in good agreement with the measurements of Schönhense,³⁰ which are shown for comparison.

The spin-polarization parameters for the ns electrons are shown in Fig. 10. For zinc the parameters are all close to their limiting nonrelativistic values of zero, except near the $3d$ threshold where

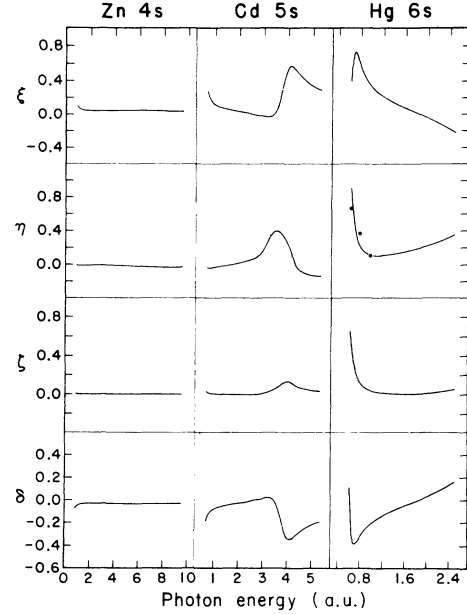


FIG. 10. Spin-polarization parameters for ns subshells. Notation is that of Huang, Ref. 27. Experiment: \bullet Schönhense *et al.*, Ref. 19.

the $4s$ Cooper minimum (which is below the $3d$ threshold in this calculation) influences their behavior slightly. The $5s$ spin-polarization parameters have a noticeable threshold energy dependence governed by the $5s$ Cooper minimum and a second region of rapid variation near 4 a.u. attributed to a second Cooper minimum. Sizable relativistic effects are also predicted for the mercury $6s$ spin-polarization parameters near the $5d$ threshold. For the mercury η parameter we also show the experimental results of Schönhense *et al.*¹⁹ for comparison. We find that the $6s$ spin-polarization parameters for mercury are large in the entire range of interest in contrast to the approximately zero values for the zinc $4s$ parameters, illustrating the rapid increase in the importance of relativistic effects with increasing nuclear charge.

V. CONCLUSIONS

There are a number of general remarks that can be made concerning the comparison between experimental and theoretical cross sections and branching ratios. First, it appears that RRPA overestimates the size of the cross sections for cadmium and mercury. The discrepancy may be due to the difficulty in determining absolute cross sections ex-

perimentally or may be, as suggested by Carter and Kelly,⁴ for cadmium and by Amusia and Cherepkov² for argon, due to the fact that the RRPA neglects the effects of core relaxation. More precise absolute cross-section measurements would certainly aid in assessing the importance of relaxation effects in group-II B elements. A second indication of the potential importance of relaxation effects is found in the comparison of branching ratios. For both cadmium and mercury we see that the experimental branching ratios near thresholds are intermediate between the relaxed but uncoupled DF predictions of Tambe *et al.*⁷ and the present unrelaxed but coupled RRPA calculation. Again more precise experimental data could help clarify the role of core relaxation. The experimental branching ratios for zinc are completely at variance with theoretical predictions and with experimental values for cadmium and mercury; further measurements of γ for zinc are clearly desirable.

Several general observations concerning the comparison between experimental and theoretical angular distributions can also be made. First, the RRPA β parameters for $(n-1)d$ electrons in cadmium and mercury are in fairly good agreement with the experimental results. It would be useful to extend the measurements to higher energies where the $(n-1)p$ electrons play a more important role to help gain an insight into the influence of the more tightly bound electrons on the outer shells. Second, the behavior of the $6s$ β parameter

for mercury in the threshold region is sensitive to the location of the $6s$ Cooper minimum. Further measurements of β_{6s} near threshold should provide a clearer picture of whether the $6s$ Cooper minimum occurs below threshold as predicted by the RRPA or above threshold as indicated by the measurements of Shannon and Codling.¹⁵ Measurements of the $5s$ β parameter in cadmium are also desirable especially near 4 a.u. to test the possible occurrence of second Cooper minimum in the $5s$ cross section. In a similar way measurements of the mercury $6s$ spin polarizations and those for the $5s$ of cadmium will be important in locating the corresponding cross-section minima. Further experimental studies of the $(n-1)d$ spin-polarization parameters for all of the group-II B elements will lead to a fuller understanding of the role of relativistic and correlation effects in these systems.

ACKNOWLEDGMENTS

The authors wish to thank S. T. Manson, J. Berkowitz, and H. P. Kelly for useful discussions. Particular thanks are also due to G. Schönhense for providing us with as yet unpublished experimental data. The work of W. R. J., V. R., and P. D. was partially supported by the NSF under Grant No. PHY79-09229. V. R. was partially supported by Research Foundation of S. R. Serbia, Yugoslavia. The work of K. T. C. was supported by the U. S. Department of Energy.

*Permanent address: Boris Kidrič Institute-Vinča, P.O.B. 522, 11001 Beograd, Yugoslavia.

¹W. R. Johnson and C. D. Lin, *Phys. Rev. A* **20**, 964 (1979); W. R. Johnson and K. T. Cheng, *Phys. Rev. A* **20**, 978 (1979).

²M. Ya. Amusia and N. A. Cherepkov, *Case Stud. At. Phys.* **5**, 47 (1975).

³A. W. Fliflet and H. P. Kelly, *Phys. Rev. A* **13**, 312 (1976).

⁴S. L. Carter and H. P. Kelly, *J. Phys. B* **11**, 2467 (1978).

⁵F. Keller and F. Combet-Farnoux, *J. Phys. B* **12**, 2821 (1979).

⁶T. E. H. Walker, J. Berkowitz, J. L. Dehmer, and J. I. Waber, *Phys. Rev. Lett.* **31**, 678 (1973).

⁷B. R. Tambe, W. Ong, and S. T. Manson, *Phys. Rev. A* **23**, 799 (1981).

⁸C. E. Theodosiou, A. F. Starace, B. R. Tambe, and S. T. Manson, *Phys. Rev. A* **24**, 301 (1981).

⁹H. Harrison, R. I. Schoen, R. B. Cairns, and K. E. Schubert, *J. Chem. Phys.* **50**, 3930 (1969).

¹⁰R. B. Cairns, H. Harrison, and R. I. Schoen, *J. Chem. Phys.* **51**, 5440 (1969).

¹¹R. B. Cairns, H. Harrison, and R. I. Schoen, *J. Chem. Phys.* **53**, 96 (1970).

¹²K. Codling, J. R. Hamley, and J. B. West, *J. Phys. B* **11**, 1713 (1978).

¹³J. L. Dehmer and J. Berkowitz, *Phys. Rev. A* **10**, 484 (1974).

¹⁴S. Süzer, P. R. Hilton, N. S. Hush, and S. Nordholm, *J. Electron Spectrosc. Relat. Phenom.* **12**, 357 (1977).

¹⁵S. P. Shannon and K. Codling, *J. Phys. B* **11**, 1193 (1978).

¹⁶H. Harrison, *J. Chem. Phys.* **52**, 901 (1970).

¹⁷A. Niehaus and M. W. Ruf, *Z. Phys.* **252**, 84 (1972).

¹⁸G. Schönhense, *J. Phys. B* **14**, L187 (1981), and private communication.

¹⁹G. Schönhense, U. Heinzmann, and J. Kessler, contributed paper, ECAP, Heidelberg, 1981 (unpublished).

²⁰G. Schönhense, contributed paper, ECAP, Heidelberg, 1981 (unpublished).

²¹H. P. Kelly, *Adv. Theo. Phys.* **2**, 75 (1968).

- ²²C. E. Moore, *Atomic Energy Levels*, Natl. Bur. Stand. (U.S.) Circ. No. 467 (U.S. GPO, Washington, D. C., 1971), Vols. II and II.
- ²³A. L. Fetter and J. D. Walecka, *Quantum Theory of Many-Particle Systems* (McGraw-Hill, New York, 1971).
- ²⁴S. Süzer, S.-T. Lee, and D. A. Shirley, *Phys. Rev. A* **13**, 1842 (1976).
- ²⁵K. Codling (private communication).
- ²⁶W. R. Johnson and K. T. Cheng, *Phys. Rev. Lett.* **40**, 1167 (1978).
- ²⁷K. N. Huang, *Phys. Rev. A* **22**, 223 (1980).
- ²⁸C. M. Lee, *Phys. Rev. A* **10**, 1598 (1974).
- ²⁹N. A. Cherepkov, *Zh. Eksp. Teor. Fiz.* **65**, 933, (1973) [*Sov. Phys.—JETP* **38**, 463 (1974)].
- ³⁰G. Schönhense (private communication).